AIAA Propulsion and Energy Forum and Exposition, July 9-11, 2018, Cincinnati, Ohio

Tuning Process for the Modified Magnussen Combustion Model

A. T. Norris *

NASA Langley Research Center, Hampton, Virginia, 23681-2199, U.S.A

In the application of CFD to turbulent reacting flows, one of the main limitations to predictive accuracy is the chemistry model. Using a full or skeletal kinetics model may provide good predictive ability, however, at considerable computational cost. Adding the ability to account for the interaction between turbulence and chemistry improves the overall fidelity of a simulation but adds to this cost. An alternative is the use of simple models, such as the Magnussen model, which has negligible computational overhead, but lacks general predictive ability except for cases that can be tuned to the flow being solved.

In this paper, a technique will be described that allows the tuning of the Magnussen model for an arbitrary fuel and flow geometry without the need to have experimental data for a particular case. The tuning is based on comparing the results of the Magnussen model and full finite-rate chemistry when applied to perfectly and partially stirred reactor simulations. In addition, a modification to the Magnussen model is proposed that allows the upper kinetic limit for the reaction rate to be set, giving better physical agreement with full kinetic mechanisms. In order to improve the agreement with flame temperatures, the thermal properties of the product species is adjusted to better match the mixture properties of the full mechanism. The combustion model is then applied to the simulation of a representative scramjet flowpath, and the results compared to experimental data and other kinetic models. This procedure allows a simple reacting model to be used in a predictive manner, and affords significant savings in computational costs for CFD simulations.

Introduction

One of the challenges of performing simulations of reacting flows is the ability to model the chemical source term. The direct approach of modeling a full set of kinetic equations is extremely expensive computationally. For example, the GRI-Mech-3.0 mechanism for methane combustion[1] consists of 53 species and 350 rate equations, which would be virtually intractable for anything but the simplest of flows. Because of the complexity of these full mechanisms, different techniques have been proposed to simplify them, and thus, reduce the computational cost. Skeletal mechanisms, reduced mechanisms and Intrinsic Low-Dimensional Manifold (ILDM) methods are examples of existing techniques that reduce the work required to evaluate the chemical source term. However, it is also known that, due to the nonlinearities of the chemical source term and fluctuations introduced by turbulence, the time averaged source terms are not being calculated exactly. Specifically, using the mean mass fractions and mean temperature to calculate the mean species source term is an approximation, i.e.,

$$\overline{S_j(Y_i, T)} \approx S_j(\overline{Y_i}, \overline{T}), \tag{1}$$

where S_j is the source term of the j-th species, Y_i is the mass fraction of the ith species, T is the temperature and the overbar denotes the average value of the quantity. Indeed it has been shown that the differences in the mean reaction rate associated with assuming equality in Eqn.(1) can be several orders of magnitude different from the exact solution.[2]

To address this issue, several models and numerical approaches have been developed in order to improve the modeling inaccuracy. Models include the Direct Quadrature Moment Method (DQMOM),[3] the Assumed Probability Density Function (PDF),[4] the Transported PDF[5] and the Linear Eddy Model.[6] All these

*Aerospace Engineer, Hypersonic Airbreathing Propulsion Branch, Senior Member AIAA.

approaches attempt to model the influence that turbulence has on chemical reaction to varying degrees of fidelity. Unfortunately, as the modeling becomes more sophisticated, there is a corresponding increase in the computational cost, especially when coupled with the added expense of chemical kinetics schemes.

One way to address the expense of kinetics modeling is to prescribe a simple method of accounting for the heat release of chemistry, and modify that to address the interaction between the turbulence and the chemistry source term. Such an approach was proposed by Magnussen in 1976,[7] and due to the simplicity of the model, the approach has proved to be very popular. However, the simplicity of the model results in several undesirable features, namely that it needs to be tuned to the flow that it is modeling and it lacks realizability in the modeled reaction rate. In addition, the fully burnt flame temperature of the Magnussen model tends to be considerably higher than that predicted by a full chemical mechanism.

Magnussen Model

Consider a chemical reaction in a homogeneous reactor, defined by the mass fraction of fuel Y_f, oxidizer Y_o and products Y_p. The rate of fuel consumption for the Magnussen model is given by:

$$\frac{d\rho Y_f}{dt} = min \begin{cases} A\,\rho Y_f/\tau_t \\ A\,\rho Y_o/\tau_t r_s \\ AB\,\rho Y_p/\tau_t(1+r_s) \end{cases} \tag{2}$$

where A and B are constants, r_s is the stoichiometric ratio of fuel to oxidizer, ρ is the density of the mixture and τ_t is the turbulent time scale. The two terms, $A\,\rho Y_f/\tau_t$ and $A\,\rho Y_o/\tau_t r_s$ give the rate of change of the fuel to be proportional to the availability of fuel or oxidizer, respectively. The constant A controls the magnitude of the rate, while the turbulent time scale in the equation models the effect of turbulence on reaction rates. As the turbulence becomes more intense, mixing of species will become more vigorous, and so a faster reaction can be sustained. The third term, $AB\,\rho Y_p/\tau_t(1+r_s)$ sets the rate of fuel consumption to be proportional to the concentration of products in the gas mixture. This term is intended to account for the effect of ignition delay and is often neglected in non-premixed reaction calculations.[8] The final reaction rate for the fuel is taken as the minimum of the three rate expressions, and the reaction rates of the other species, ρ_o and ρ_p, are simply proportional to the fuel reaction rate.

$$\begin{aligned} \frac{dY_o}{dt} &= r_s \frac{dY_f}{dt} \\ \frac{dY_p}{dt} &= -(1+r_s)\frac{dY_f}{dt} \end{aligned} \tag{3}$$

An illustration of the Magnussen model is shown in Fig.1 where the reaction rate of the product species is plotted against the mass fraction of the products for a stoichiometric mixture of fuel and oxidizer. The first two parts of Eqn.(2) describe the part of the curve to the right of the peak value, while the third part of the equation gives the curve to the left of the peak. The value of Y_p at which the peak reaction rate occurs is determined by the value of B, where a value of 1 would give a peak value at $Y_p = 0.5$. The effect on the reaction rate due to changing the value of the turbulent time scale is also shown, with the reaction rate increasing inversely proportional to the increase in τ_t. It should be noted that the shape of the reaction rate in Fig.1 crudely matches what one would expect if the reaction rate of fuel, oxidizer or product obtained from a full mechanism was plotted against the mass fraction of that species (Fig.(2))

The Magnussen model has a few issues that limit its effectiveness. First, it is not predictive. The model needs to be tuned to individual geometries, conditions and fuels. Second, the model accounts for the interaction of turbulence and chemistry by simply making the reaction rate inversely proportional to the turbulence time scale. While for a certain range of time scales this is a reasonable approximation, chemical reactions do have an upper limit for the speed of reaction. Once that limit is reached, no matter how quickly the flow is mixed, the chemistry will not react any faster. Yet the Magnussen model does not have such a limit. As the turbulent time scale goes to zero, the resulting reaction rate obtained from the Magnussen model approaches infinity. Another issue is that the adiabatic flame temperature is often over-predicted by a reduced mechanism, such as the Magnussen model. This is because the notional species used in the Magnussen model are in effect representing the properties of a mixture of species, and consequently the thermal properties of these notional species need to be adjusted. Consider the fuel species for example. In a full mechanism one of the first steps is to break down the fuel molecules into smaller components, so

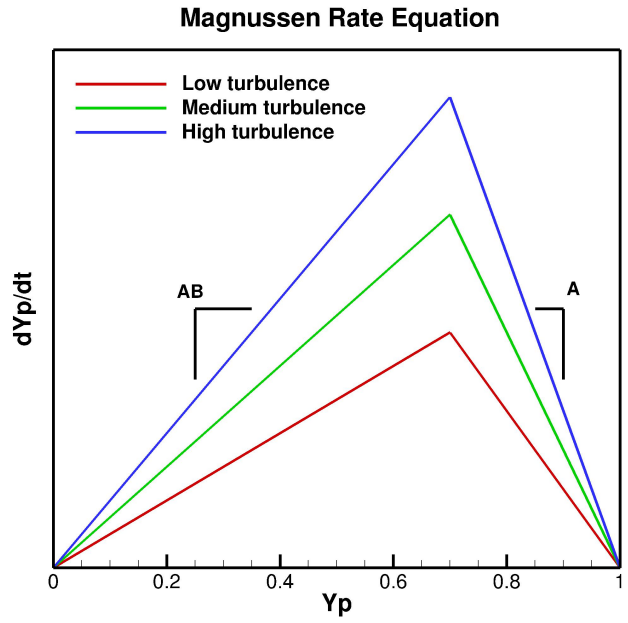

Figure 1. The rate of product creation dY_p/dt plotted against the product mass fraction Y_p showing the effect of varying turbulence time scale on the reaction rate.

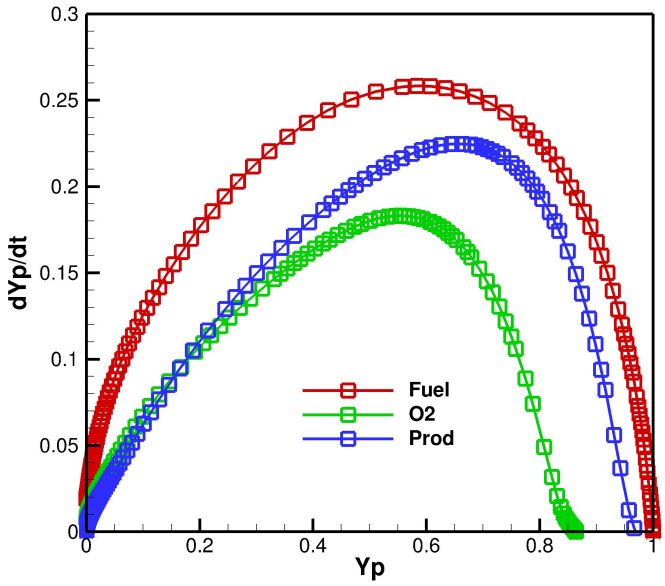

Figure 2. The rate of product creation dY_p/dt plotted against the product mass fraction Y_p obtained from full mechanism. Normalized product creation rate is based on fuel, oxidizer and product mass fractions shown.

the quantity of fuel in the mixture reduces quickly. However in the Magnussen model, the fuel transforms directly into product, and so a fraction of the fuel molecules remain in the mixture throughout the combustion process, thus the thermal properties of the mixture needs to be corrected.

To address these issues, it is proposed that the Magnussen model be tuned against simple canonical reaction simulations, where the use of a full chemical mechanism is tractable, and extrapolate those results to a real flow situation. The simple canonical cases proposed are the Perfectly Stirred Reactor (PSR) and the Partially Stirred Reactor (PaSR). These two cases were chosen because they represent a single cell in a finite volume CFD code (PSR) and a single cell of a Eulerian Probability Density Function (PDF) transport code (PaSR). In addition, an adapted Magnussen model will be proposed to address the issue of having a potentially infinitely fast reaction rate. The process involved in tuning the model and limiting the rate has been addressed in a previous paper,[9] however this work extends the methodology. In this paper, the chemical kinetics of a surrogate cracked JP7[10] and air reaction will be considered and used to tune the Magnussen model. The cracked JP7 chemical mechanism is represented by a reduced mechanism of 32 species and 206 rate equations.[11] This mechanism is representative of the sort of complex hydrocarbon kinetics that represent the chemistry of a scramjet combustor. The process of adjusting the thermal and transport properties of the synthetic Magnussen model species will then be described and the resulting reaction kinetics will be applied to the HIFiRE Direct-Connect Rig (HDCR)[12,13] scramjet flowpath.

Tuning

Consider a single computational cell in a finite-volume CFD solution with chemical reaction (Fig.3) where

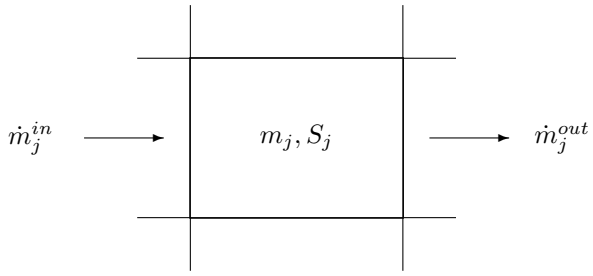

Figure 3. Schematic of single computational cell in a finite volume CFD solution.

m_j is the mass of species j contained in the cell and S_j is the rate of creation of species j due to chemical reaction. Also shown is the mass flow rate of species j entering the cell, $\dot{m}_j^{in}$ and the mass flow rate leaving the cell, $\dot{m}_j^{out}$. The change in the mass of species j contained in the cell as a function of time is given by

$$\frac{dm_j}{dt} = S_j + \dot{m}_j^{in} - \dot{m}_j^{out}. \tag{4}$$

For a steady state situation, which would correspond to a steady state CFD solution, the left hand side of Eqn.4 is zero, and it is apparent that there is a strong resemblance between this single cell and a Perfectly Stirred Reactor, (PSR). The mass contained in the cell, divided by the mass flow rate into the cell gives a residence time, τ_r for the volume. In a PSR, and also a single cell in a finite volume scheme, as the mass flow rate into the reactor increases, the residence time decreases and the mass fraction of products of combustion start to drop off. When the inflow becomes sufficiently large, the reaction is unable to be sustained, and the reactor is said to have blown out. For a given volume, the reactor can be parameterized by just the residence time and reaction rate.

Likewise, consider a single cell in an Eulerian PDF simulation as shown in Fig.4. The composition in the cell is represented by a probability distribution of different values of scalars, $\mathcal{F}$, which evolves due to molecular mixing, M, chemical reaction, S and the inflow and outflow of distributions of scalars j, given by $\dot{\mathcal{F}}^{in}$ and $\dot{\mathcal{F}}^{out}$ respectively. The evolution of the distribution of all the scalar quantities in the cell, $\mathcal{F}$, as a function of time is given by

$$\frac{d\mathcal{F}(\vec{\psi},t)}{dt} = \sum_{j=1}^{N_s} \frac{d}{d\psi_j}[M_j(\vec{\psi},t) + S_j(\vec{\psi},t)]\mathcal{F}(\vec{\psi},t) + \dot{\mathcal{F}}^{in}(\vec{\psi}) - \dot{\mathcal{F}}^{out}(\vec{\psi}) \tag{5}$$

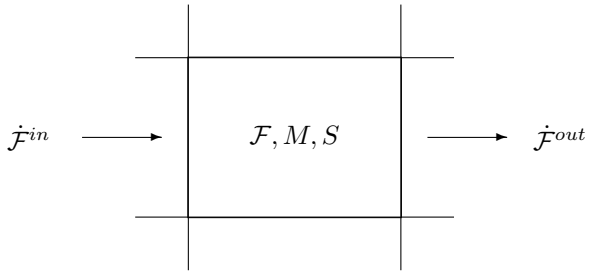

Figure 4. Schematic of a single computational cell in an Eulerian Probability Density Function simulation.

where the ψ_j represents the scalar space of species j and temperature, and the number of scalars is given by N_s. In a similar way as with the PSR, if the change of the distribution of scalars with time is zero, corresponding to a steady state solution, the computational cell can be considered to behave the same as a Partially Stirred Reactor, (PaSR). Like the PSR, the PaSR is parameterized by a residence time scale and a reaction time scale, but also has a turbulent mixing time scale, τ_t. When simulating the PaSR model it is also helpful to define the ratio of the residence time and the mixing time scale as a constant value. That is,

$$Da = \frac{\tau_t}{\tau_r} \tag{6}$$

where τ_t and τ_r are the turbulence and residence time scales, respectively.

Using the two reactors described above, and observing that the Magnussen model has a simple turbulence-chemistry interaction model as part of its makeup, the tuning process proposed involves solving the PaSR reactor with the full mechanism, and then using the results to tune the Magnussen model, run in the PSR mode. That way the performance of the simple turbulence-chemistry interaction model can be tuned against the physically exact model used by the full mechanism.

For the chemical mechanism used in this paper, the fuel consists of a mixture of CH4 and C2H4. The properties of the synthetic fuel species, Y_f, are given by mixture relations. For example, the mixture specific heat at a given temperature, $\overline{Cp(T)}$, is given by

$$\overline{Cp(T)} = \sum_{k=1}^{Ns} Cp_k(T) Y_k \tag{7}$$

where Y_k is the mass fraction of species k and $Cp_k(T)$ is the specific heat of species k at temperature T. The values of $Cp_k(T)$ are commonly represented by a polynomial fit developed by Gorden and McBride.[14] The properties of the oxidizer are those of O2, and typically the product is represented by the combination of $CO2$ and $H2O$ in stoichiometric proportion. However, for the product, evaluating the specific heat in this manner leads to an over-prediction of the fully burnt temperature since dissociation is neglected. This topic will be further discussed later.

Application

The geometry for testing the modified Magnussen model will be the HDCR flow geometry, shown in Fig.5. In the simulations performed in this paper, the geometry has been simplified to enable simulations using a full chemistry mechanism. As a result, the modeled configuration is a slice containing two injectors, as shown in Fig.6. To ensure the full mechanism could be run in a reasonable time, the grid resolution was made very coarse, with the total domain being composed of only about 350,000 cells. Because of this, comparison with experimental data was not considered valid, whereas the comparisons between the full mechanism and the Modified Magnussen model are deemed appropriate.

The first part of the tuning process is to select the conditions that are representative of the flow. For the HDCR case, this is the total temperature of the fuel and air inflows and a pressure that is representative of

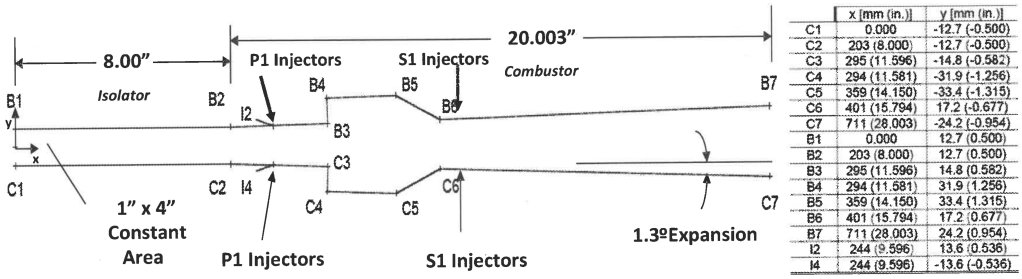

	x [mm (in.)]	y [mm (in.)]
C1	0.000	-12.7 (-0.500)
C2	203 (8.000)	-12.7 (-0.500)
C3	295 (11.596)	-14.8 (-0.582)
C4	294 (11.581)	-31.9 (-1.256)
C5	359 (14.150)	-33.4 (-1.315)
C6	401 (15.794)	17.2 (-0.677)
C7	711 (28.003)	-24.2 (-0.954)
B1	0.000	12.7 (0.500)
B2	203 (8.000)	12.7 (0.500)
B3	295 (11.596)	14.8 (0.582)
B4	294 (11.581)	31.9 (1.256)
B5	359 (14.150)	33.4 (1.315)
B6	401 (15.794)	17.2 (0.677)
B7	711 (28.003)	24.2 (0.954)
I2	244 (9.596)	13.6 (0.536)
I4	244 (9.596)	-13.6 (-0.536)

Figure 5. Internal lines of the HDCR flowpath.

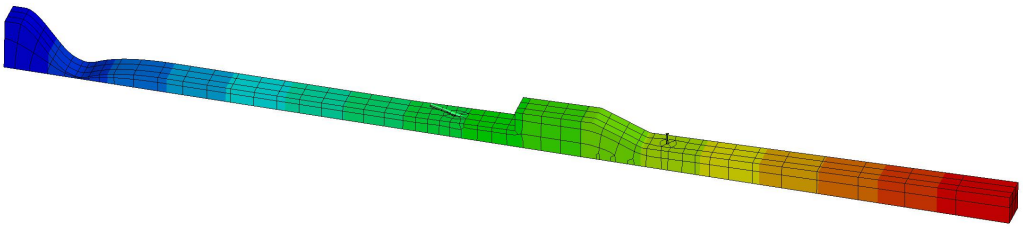

Figure 6. Computational domain based on part of the HDCR flowpath.

the combustor pressure. The total temperature was chosen because a significant amount of reaction occurs in cavity and flame holding regions where the flow is subsonic. In this case, the total temperatures for the fuel and air inflow were 298K and 2800K, respectively, while the pressure was set at 1.5 atmospheres. Using these values, the PaSR was run for various residence times, and for a variety of Da numbers. The results are shown in Fig.7. The first observation is that the effect of the Da number on the reactor is significant. This factor is a measure of the effect of turbulence-chemistry interaction, as high Da numbers, ($Da > 10$), correspond to fully burnt results, while low Da numbers, ($Da < 1$), correspond to mixing-limited reaction. The second observation is that the residence time where the reactor is unable to sustain chemical reaction is similar for different values of Da.

The results of running the Magnussen model in the PSR with the same inflow conditions and pressure as the PaSR are shown in Fig.8. The first observation is that because the reaction rate has no upper limit, the temperature plots are constant for a given Da number. This is because a constant Da number has the reactor residence time proportional to the reaction time of the Magnussen model. As the Da number approaches a large number, the temperature asymptotes to a constant value which represent a fully burnt state. Conversely, as the Da number approaches zero, the reaction time is much greater than the residence time and so the temperature approaches the mixed, unreacted state. Note that for a finite rate mechanism in a PSR, the reaction rate is not a function of ϵ/k, and so the PSR result would yield only a single temperature curve. The other observation to be made about the results in Fig.8 is that the temperature predicted for each Da number is considerably higher than the value of the equivalent Da number in the PaSR result for the full mechanism. These results illustrates two shortcomings of the existing Magnussen model, namely the temperatures are over-predicted and that there is no reaction cut-off below a certain residence time.

The thermal properties of the Magnussen model components need to be adjusted to resolve the first shortcoming. The fuel and oxidizer need not be changed, but the product specific heat needs to be adjusted to account for the temperature over-prediction. For the existing Magnussen model, the thermal properties of the product are simply obtained by considering the reaction:

$$9CH4 + 16C2H4 + 66O2 => 41CO2 + 50H2O \tag{8}$$

Thus, the thermal properties are obtained by combining the thermal properties of $CO2$ and $H2O$ in the

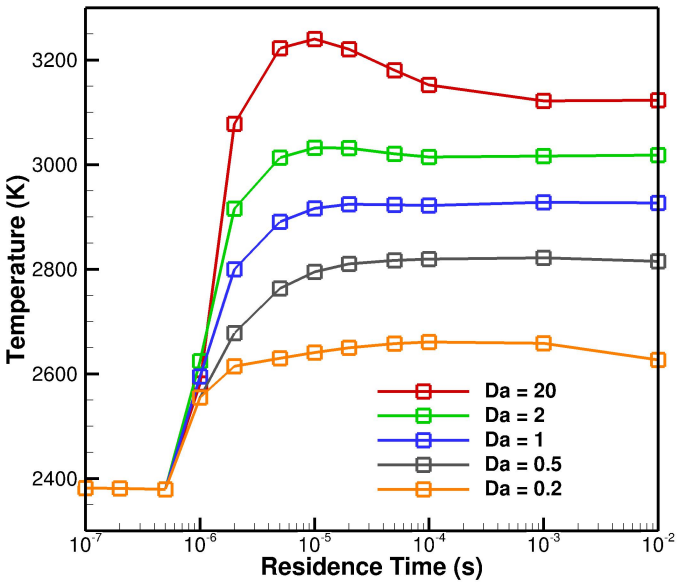

Figure 7. Reactor temperature plotted against residence time for the full mechanism PaSR simulation.

stoichiometric proportion, and the results show a significant over-prediction of the temperatures. To overcome

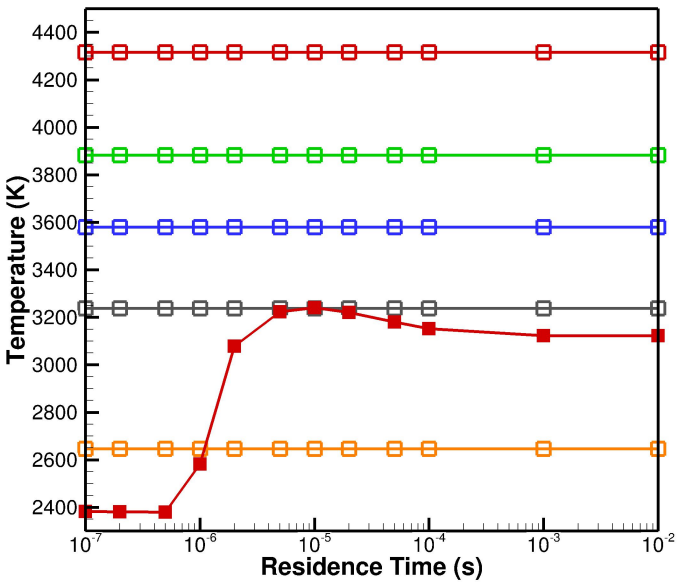

Figure 8. Reactor temperature plotted against residence time for the baseline Magnussen model, with no adjustment to the value of $Cp_P(T)$. Open symbols correspond to the same Da number as in Fig.7. Solid symbol line shows the full mechanism Da = 20 results that should match the red open symbol line.

this, the proposed method is to modify the product $\overline{Cp_P(T)}$ polynomial function so that it returns a higher

value and effectively results in the product requiring more energy to increase the temperature. To do this, the linear temperature constant in the polynomial is adjusted by a factor a_f to give the new value of $\hat{Cp_P}(T)$

$$\frac{\hat{Cp_P}(T)}{R} = a_1 + (a_2 + a_f)T + a_3T^2 + a_4T^3 + a_5T^4 \tag{9}$$

Correspondingly, the extra term in the enthalpy polynomial is then adjusted to keep the heat of formation unchanged. The value of the adjustment factor a_f is obtained by trial and error using the standard Magnussen model and matching the high Da lines at large residence times with the PaSR result. The resulting factor for this case was found to be $a_f = 2.74 \times 10^{-3}$.

Once the value of $\hat{Cp_P}(T)$ has been set, the two Magnussen constants, A and B can be set. Constant A is adjusted so the spacing between the $Da > 1$ lines at high residence time match those of the PaSR result. The B constant is used to adjust the $Da < 1$ lines, but the results are less sensitive to the values chosen for this constant. The result for the HDCR case is shown in Fig.9 where $A = 1.5$ and $B = 2.0$.

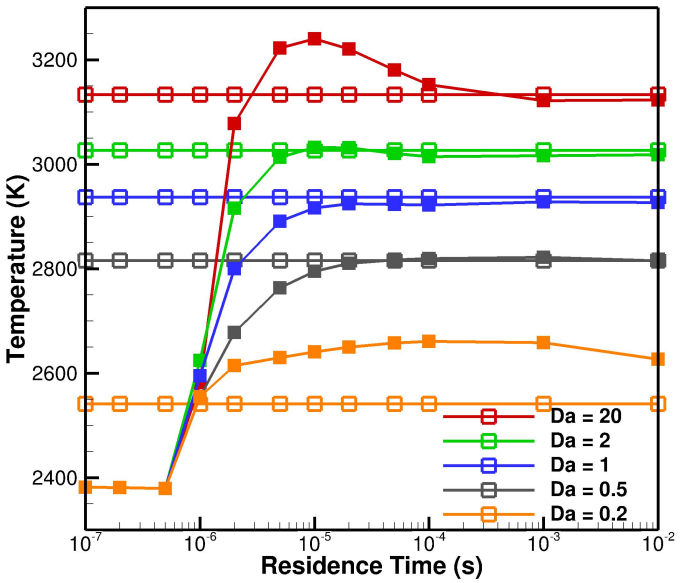

Figure 9. Reactor temperature plotted against residence time for the baseline Magnussen model, with adjusted $\hat{Cp_P}(T)$ and rate constants adjusted. Solid symbols shows full mechanism PaSR results that should match the open symbol lines of corresponding color.

Having established the new product $\hat{Cp_P}(T)$ and the two Magnussen model constants, the next item to address is the Magnussen model having no upper reaction limit. A simple solution to this is to modify the Magnussen model by establishing a limit on the value that τ_t can take and thus ensuring that the reactor will eventually blow out at small enough residence times. To obtain this limit, $\hat{\tau}_t$, the $Da = 20$ curve from the PaSR is compared to the $Da = 20$ curve of the Magnussen model with different cutoff times. The results are shown in Fig.10, and while the slope of the blowout is not predicted well, a reasonable approximation is given to the blowout process. The value of $\hat{\tau}_t$ was chosen as 1.0×10^{-5}. Putting all the adjusted and tuned constants together gives the result shown in Fig.11. Comparing this result to the full mechanism result shown in Fig.7 shows that the Modified Magnussen Model (M3) can be tuned to give a good approximation to the full PaSR model. Moreover, by appealing to the similarity between a finite volume CFD cell and the reactor models, it can be presumed that the results of a CFD simulation using the Modified Magnussen model will approximate the values given by a full mechanism with the interaction of turbulence and chemistry accounted for.

One variation that has been made to the M3 is to remove the turbulence-chemistry interaction component. This is accomplished by replacing the τ_t term with the upper limit $\hat{\tau}_t$ established earlier. This has the effect

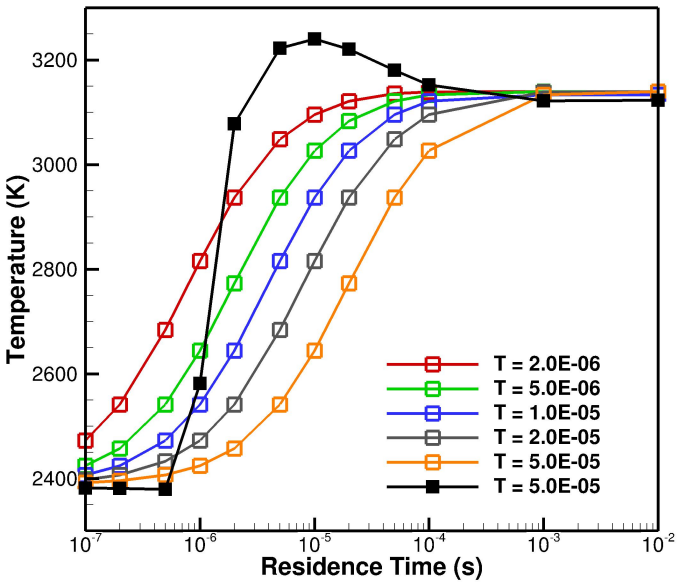

Figure 10. Reactor temperature plotted against residence time for the baseline Modified Magnussen model, with adjusted $\widehat{Cp_P}(T)$ and tuned rate constants for different values of the turbulent mixing time scale limit. Solid line shows the Da = 20 result from the full mechanism.

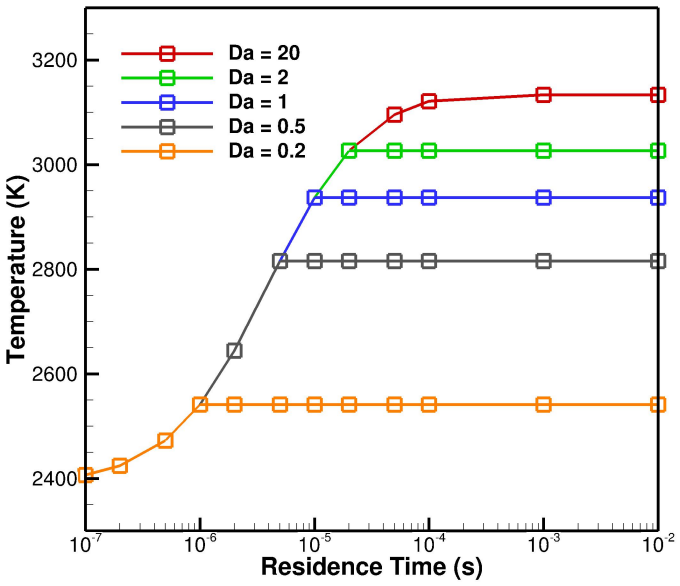

Figure 11. Reactor temperature plotted against residence time for the Modified Magnussen Model, with adjusted $\widehat{Cp_P}(T)$, tuned rate constants and tuned mixing time scale limit.

of reducing the M3 to a laminar chemistry approximation and thus gives a more direct comparison to a full mechanism simulation with no turbulence-chemistry interaction. This variation of the M3 is referred to as

the Laminar Modified Magnussen Model, LM3.

HDCR

In the previous section, the M3 was developed and a process of tuning against a full mechanism using simple reactor models was outlined. In this section, the tuned model will be applied to a realistic, albeit simplified, scramjet geometry to see how well the tuning process works when applied to a real CFD problem. In order to make a consistent comparison, the full mechanism species were post processed into fuel, oxidizer, product and dillutant mass fractions. The fuel was the sum of the two fuel components, CH4 and C2H4 while the oxidizer was the O2 mass fraction. The product was the combination of the H2O, CO2 and CO mass fractions and everything else was put in the dillutant mass fraction, for which the major component was N2. The timing of the the full mechanism run compared to the M3 and LM3 simulations was evaluated also, with the reduced models running 56 times faster than the full mechanism case.

The first comparison to be made is between the LM3 and the full mechanism simulation because the full mechanism could not be run with a turbulence-chemistry interaction model. The temperature results of the two simulations are shown in Fig.12 for a slice through the center of the injector plane as well as a plot showing the difference between the two fields. It can be seen that there is not much difference between the two temperature fields for the majority of the flow field. The biggest difference is where the LM3 has some reaction occurring along the first injector stream whereas the full mechanism does not. This is not unexpected as the physics of ignition delay are not represented by the LM3 and this is an area that does not have a flame holding region in close proximity. The other quantity of interest is the pressure field and the comparison between the LM3 and the full mechanism for this quantity is shown in Fig.13. In general the pressure fields show little difference except for a few peaks near the centerline and at the exit of the combustor section. These peaks seem to correspond to shock structures, so it is reasonable to infer that the changes in the thermal properties due to excess burning in the LM3 model may contribute to the difference in pressure after shocks. It should be noted that the change in pressure at the exit of the combustor region does not extend more than a few centimetres beyond the region shown, and it is postulated that the full mechanism is burning more fuel in this region. Overall, the comparison between the two simulations is rather good, considering the difference in the complexity of the models.

In an effort to quantify the difference between the two flow fields, the difference between the two computational domains was averaged for each cell with an axial location greater than 20 centimetres downstream of the throat. This location was chosen as the cells upstream of this point have negligible differences. The comparison of quantities are shown in Table1. What is observed is that on average the LM3 model is over-predicting the full mechanism temperature by about 2.0%, while under predicting the pressure by a similar percentage. The product mass fraction is over-predicted by the LM3 model, though this is to be expected as the definition of product for the full mechanism used in this paper does not include all possible species and so results in an under-predicted mass fraction.

Table 1. Difference between the LM3 and full mechanism results averaged over all cells with axial localtion greater than 0.2.

Difference	Mean	SD	% of Maximum
Temperature(K)	68.0	158.0	2.4
Pressure (atm)	-0.041	0.111	-2.0
Product (Mass frac)	0.0164	0.0327	7.1

The next comparison made is between the LM3 and the M3 and the centerline temperature fields are shown in Fig.14. Of interest in this comparison is that the effect of turbulence on reaction is to significantly reduce the amount of reaction occurring at the primary injector, which is in agreement with the finite rate mechanism. However this result is due to the turbulence-chemistry model suppressing reaction in a region where it should not be occurring, rather than matching the full mechanism results. In addition, there is a difference near the secondary injector, where the reaction is occurring behind the jet of fuel, rather than on the leading face of the jet. This is analogous to the region above the primary injector, where the M3 model is suppressing the reaction compared to the laminar chemistry model, and may represent a trend for the effect of the interaction of turbulence and chemistry.

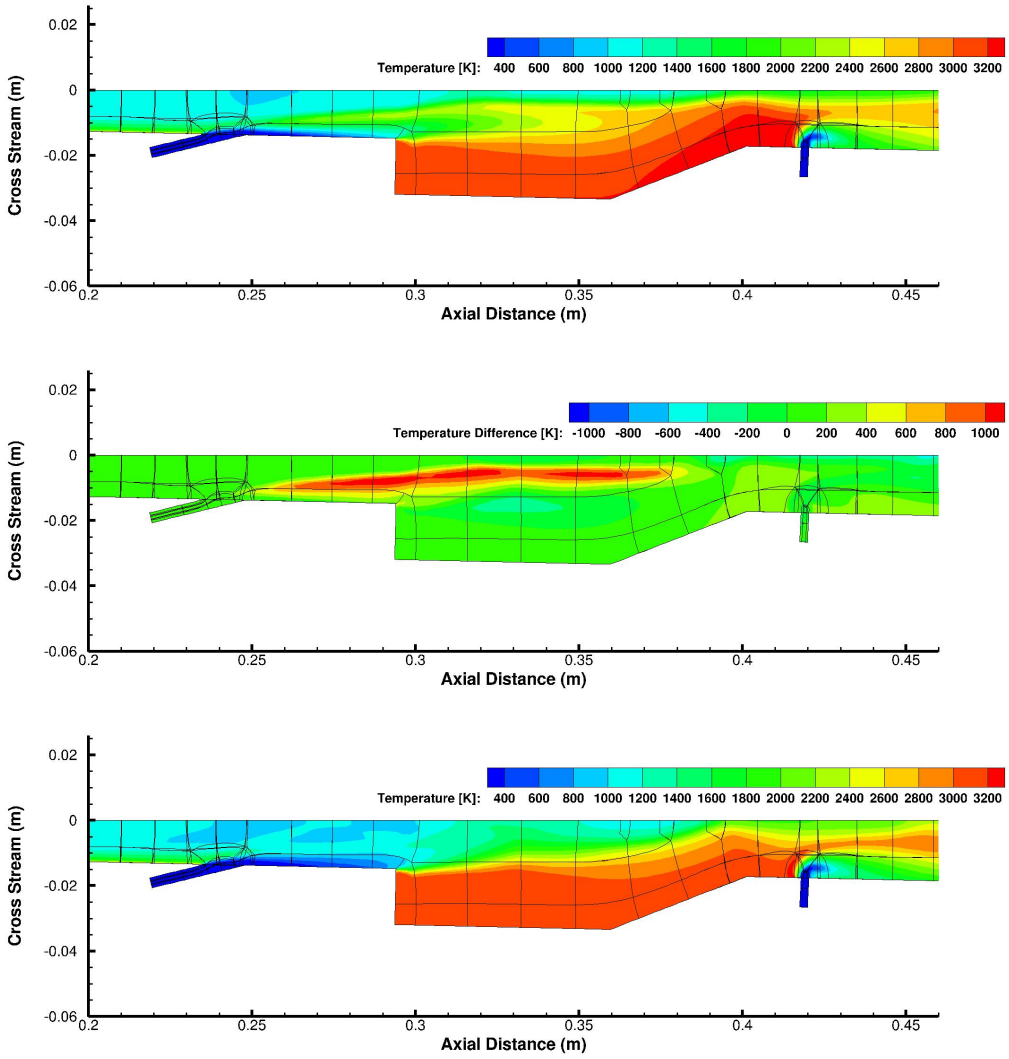

Figure 12. LM3 model temperature results (top) and full mechanism temperature results (bottom) for center line slice. Center plot shows difference between the two fields (LMS-Full).

The difference between the pressure fields (Fig.15) is more significant than the difference between the LM3 and the full chemical reaction results. The entire cavity region is at a lower pressure for the turbulent-chemistry interaction model prediction, and the small regions of pressure increase have changed. This may be caused by the reduced reaction rate predicted by the interaction of turbulence and chemistry lowering the heat release at the cavity exit and thus reducing the cavity pressure. The difference between the two domains was also calculated, and is shown in Table2. What is observed is that including a model for the interaction between turbulence and chemistry results in a decrease in the mean predicted temperature and pressure in the flow field, while there is an increase in the product mass fraction. This observation indicates that the effects of the turbulence-chemistry interaction on the flow field are going to be significant and comparable in size to the effects of the difference between a full mechanism and the LM3.

One other useful comparison to make is the difference between the baseline Magnussen result (run in laminar form) and the full mechanism simulation. The results of this are shown in Table 3. The most noticeable observation is the big differences among the predictions of the state variables between the two models, with values on the order of 10%. The difference in the product mass fraction is comparable to the tuned result, but the differences between the state variables are important as these directly impact the predicted performance of the engine.

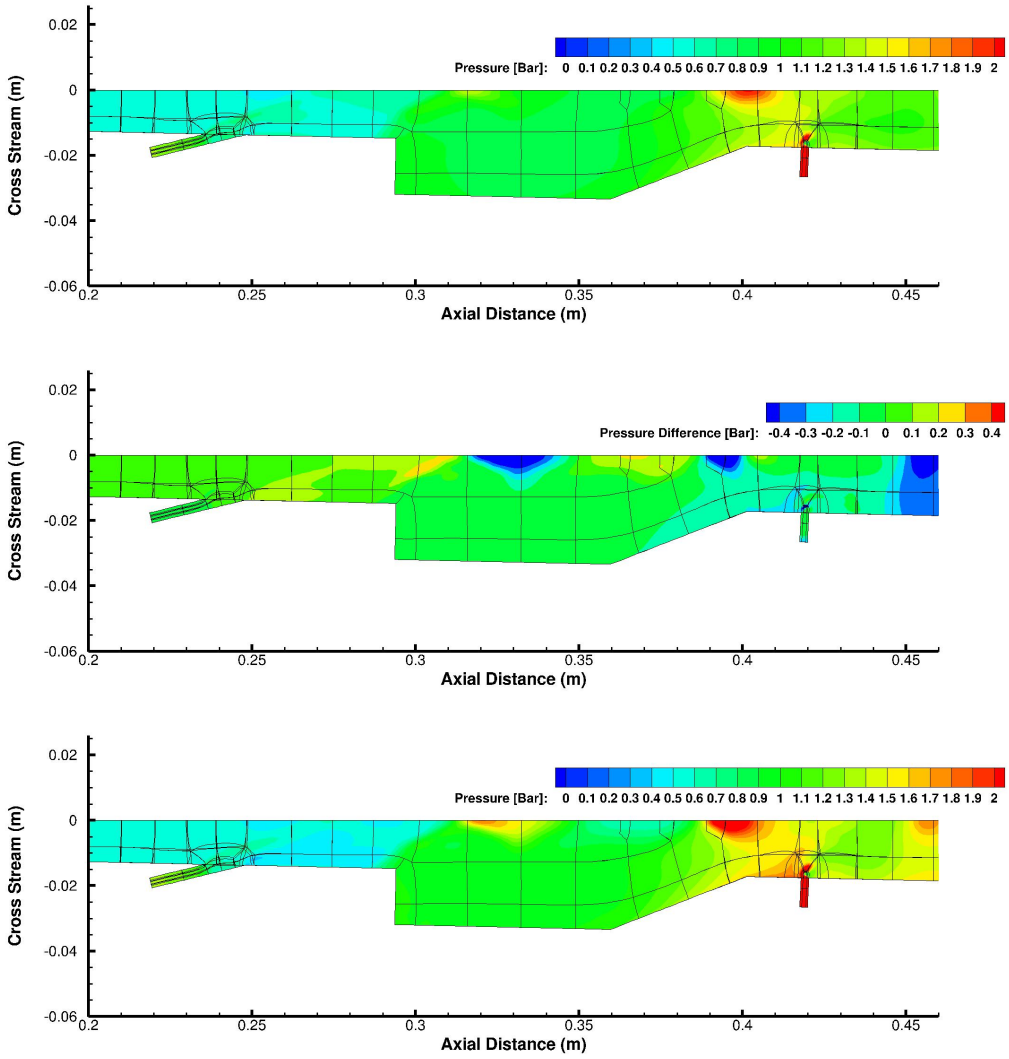

Figure 13. LM3 model pressure results (top) and full mechanism pressure results (bottom) for center line slice. Center plot shows difference between the two fields (LMS-Full).

It is also useful to look at some of the integrated, or 1D results, for this simulation to provide a view of the overall performance of the engine flowpath. For these quantities, the mass-flux averages of the properties were calculated as a function of the axial location. Shown in Figs. 16, 17 and 18 are the mass-flux averaged pressure, temperature and O2 mass fraction, respectively, as a function of axial distance. In all three plots, it can be observed that the full mechanism and the LM3 model results are in reasonable agreement, while the M3 model differs further from the finite rate model. Without a full mechanism simulation with a turbulence-chemistry model included, it is difficult to make any firm conclusions comparing the full mechanism simulation and the M3 model. However, the comparison between the M3 and the LM3 models suggest that the effects of the turbulence-chemistry interaction are not negligible and it is not obvious that this physical effect can be ignored for scramjet simulations.

The final quantity to be compared is the stream thrust of the HDCR flowpath for each combustion model at the exit plane of the flowpath and the results are shown in Table4. The comparisons show that the tuning process described in this paper gives results in very good agreement with the full mechanism predictions but at less than 2% of the computational cost. The results also show that using the existing Magnussen model without a reaction limit and unchanged thermal properties does not provide such a good agreement with the full mechanism results.

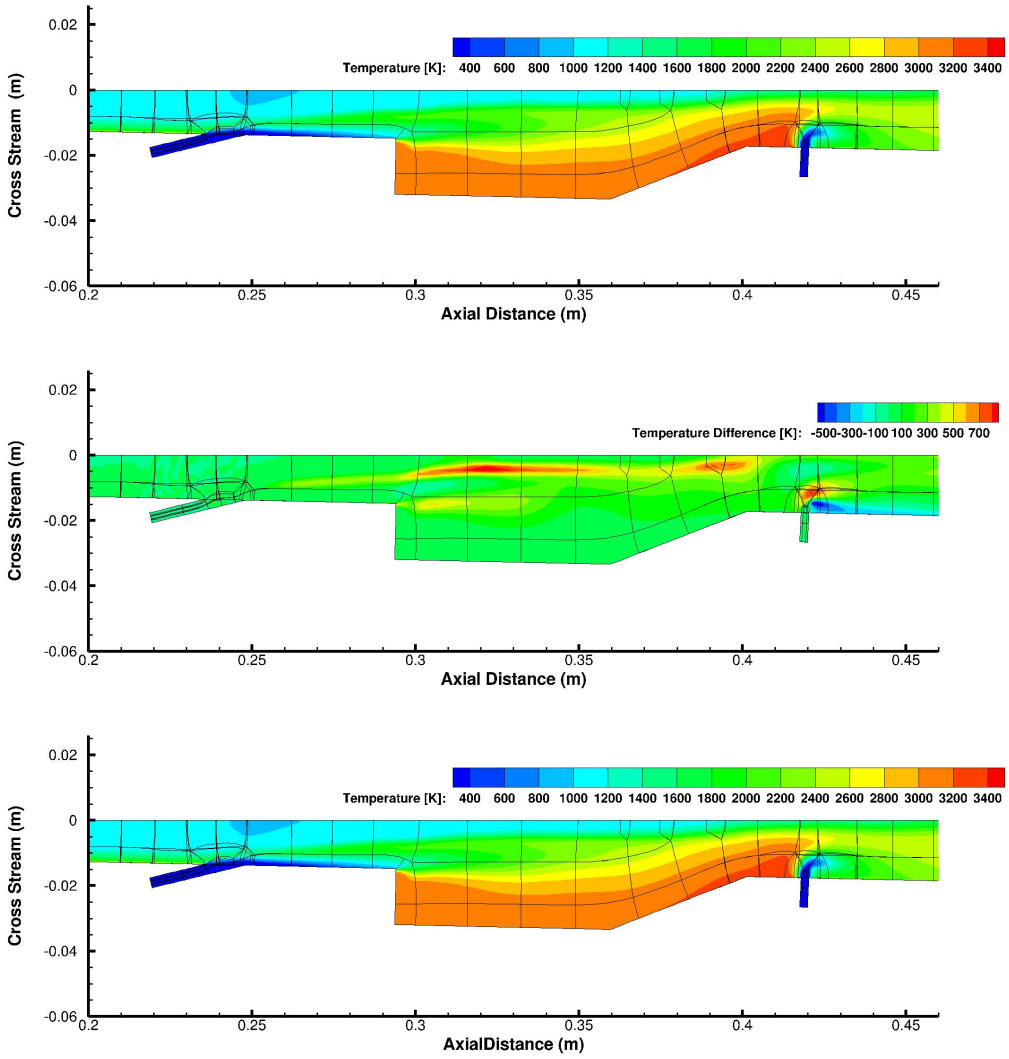

Figure 14. LM3 model temperature results (top) and M3 temperature results (bottom) for center line slice. Center plot shows difference between the two fields (LM3-M3).

Summary

In this paper, a method was proposed that would allow a modified version of the Magnussen model to be employed in a more predictive manner. Using simple reacting flow simulations of perfectly and partially stirred reactors, the Magnussen model was tuned to behave like the full mechanism. In addition, a process of determining the thermal properties of the Modified Magnussen model synthetic species was described, and the model was demonstrated by applying it to the simulation of the simplified HDCR flowpath and comparing the results to a simulation using the full chemical kinetic model. Results show that the process of using the PaSR and PSR to obtain the tuned constants provides a reasonably good predictive ability compared to that of using a full mechanism. Taking the difference between results show that the tuned Modified Magnussen Model gives very similar results to the full mechanism, with mean differences in pressure and temperature of about 2% over the entire reacting flow field. In addition, the comparison between the Modified Magnussen Model the results from a simulation with the turbulence-chemistry interaction model turned off show that the effect of the interaction between chemistry and turbulence is not negligible. Comparisons of the stream thrust at the flowpath exit plane show that the M3 and LM3 models provide a very good agreement with the full mechanism results, but at a couple of orders of magnitude less computational cost.

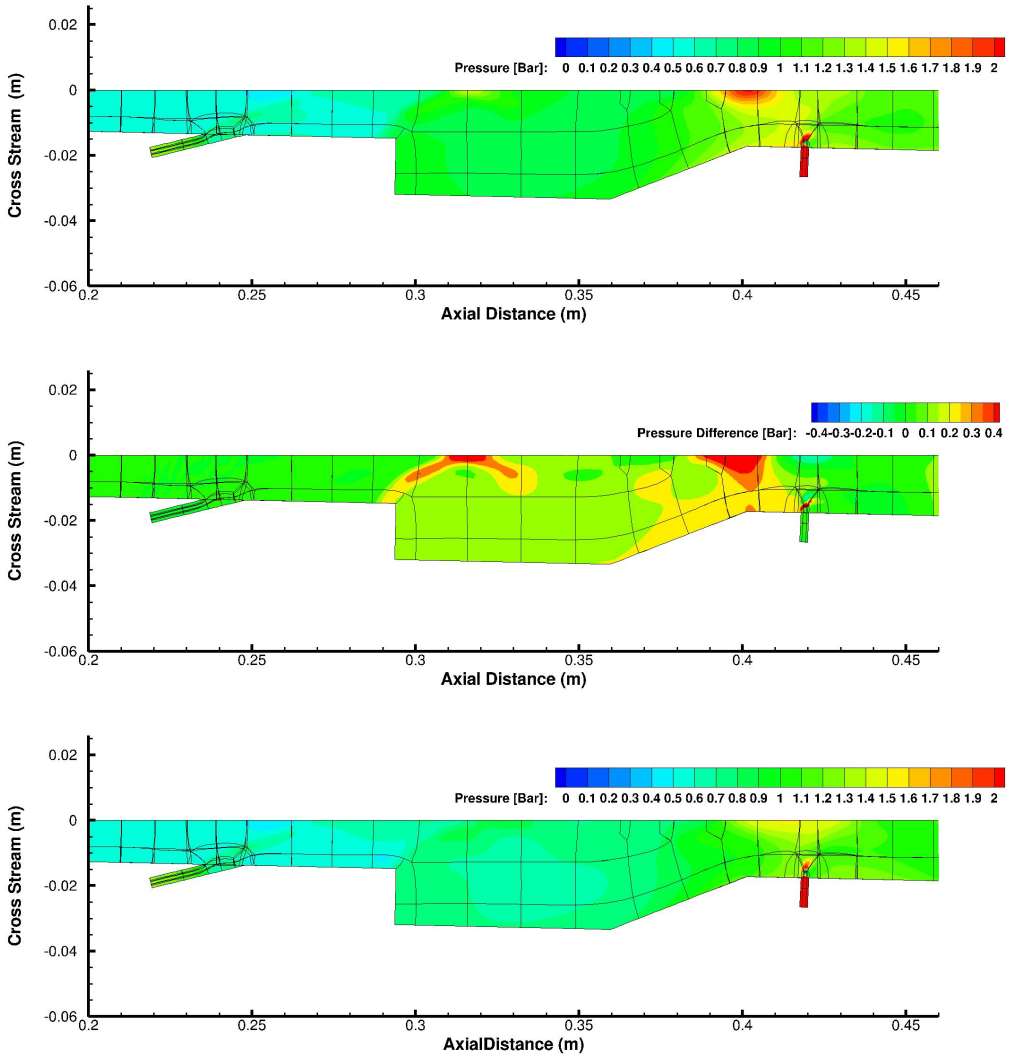

Figure 15. LM3 model pressure results (top) and M3 pressure results (bottom) for center line slice. Center plot shows difference between the two fields (LM3-M3).

The main impact of this tuning process is no further tuning is required when there is a new geometry with no experimental data available. The process described in this paper will allow a Modified Magnussen Model to be tuned to the expected conditions in the flowpath, to provide results that are comparable to those of a full mechanism, but at a fraction of the computational cost. In addition, by including a turbulence-chemistry model an important physical mechanism can be incorporated.

Table 2. Difference between the LM3 and M3 results averaged over all cells with axial localtion greater than 0.2.

Difference	Mean	SD	% of Maximum
Temperature(K)	64.0	121.0	2.3
Pressure (atm)	0.056	0.107	2.8
Product (Mass frac)	-0.010	0.0167	4.3

Table 3. Difference between the LM3 and M3 results averaged over all cells with axial localtion greater than 0.2.

Difference	Mean	SD	% of Maximum
Temperature(K)	361.0	466.0	12.7
Pressure (atm)	0.155	0.282	7.8
Product (Mass frac)	-0.016	0.0366	6.9

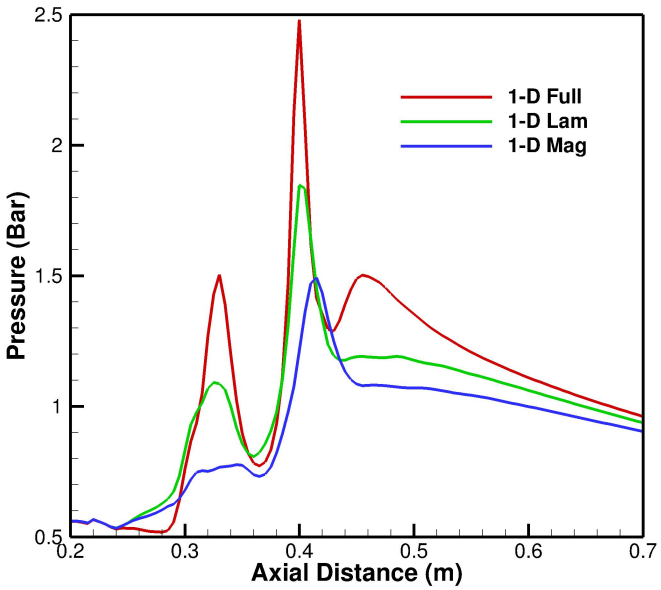

Figure 16. Cross-stream mass averaged pressure results for the Full mechanism, LM3 and M3 simulations plotted against axial distance.

References

[1]Smith, G. P., Golden, D. M., Frenklach, M., Moriarty, N. W., Eiteneer, B., Goldenberg, M., Bowman, C. T., Hanson, R. K., Song, S., William C. Gardiner, J., Lissianski, V. V., and Qin, Z., `http://www.me.berkeley.edu/gri_mech/`, Accessed 2016-03-01.

[2]Norris, A. T. and Hsu, A. T., "Comparison of PDF and Moment Closure Methods in the Modeling of Turbulent Reacting Flows," *30th AIAA/ASME/SAE/ASEE Joint Propulsion Conference, Indianapolis, Indiana*, 1994, pp. AIAA–94–3356.

[3]Fox, R. O., *Computational Models for Turbulent Reacting Flows*, Cambridge University Press, Cambridge, 2003.

[4]Janicka, J., Kolbe, W., and Kollmann, W., "Closure of the Transport Equation for the Probability Density Function of Turbulent Scalar Fields," *J. Non-Equilib. Thermodyn.*, Vol. **4**, 1979, pp. 47–66.

[5]Pope, S. B., "PDF Methods for Turbulent Reactive Flows," *Prog. Energy Combust. Sci.*, Vol. **11**, 1985, pp. 119–192.

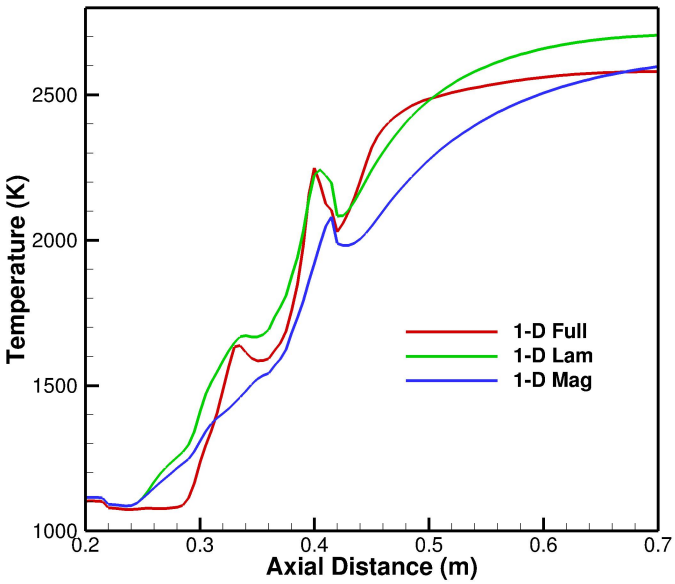

Figure 17. Cross-stream mass averaged temperature results for the Full mechanism, LM3 and M3 simulations plotted against axial distance.

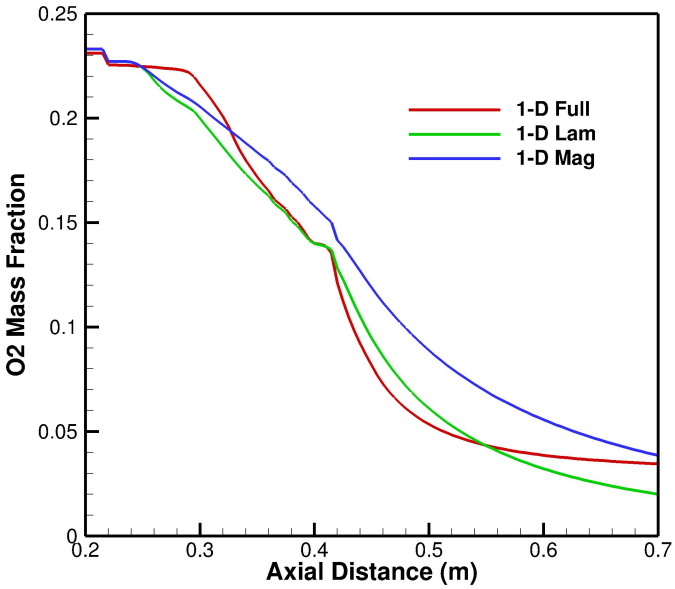

Figure 18. Cross-stream mass averaged oxygen mass fraction results for the Full mechanism, LM3 and M3 simulations plotted against axial distance.

[6]Kerstein, A. R., "A linear eddy model of turbulent scalar transport and mixing," *Combust. Sci. Tech.*, Vol. **60**, 1988, pp. 391–421.

[7]Magnussen, B. F. and Hjertager, B. H., "On Mathematical Modeling of Turbulent Combustion With Special Emphasis

Table 4. Stream thrust measured at the flowpath exit.

	Pressure Force (N)	Momentum Force (N)	Total Force (N)
Full Mechanism	58.29	202.9	261.2
LM3	56.87	203.6	260.5
M3	54.94	204.4	259.3
Magnussen Baseline	26.9	209.2	236.1

on Soot Formation and Combustion," *Sixteenth Symposium (International) on Combustion*, 1976, pp. 719–729.

[8]Norris, A. T., Jentink, T. N., Eklund, D. R., Hagenmaier, M. A., and Cox-Stouffer, S. K., "CFD Analysis of the SED SJX61-2 Engine: Comparison to Experimental Data," *JANNAF 44th Combustion, 32nd Airbreathing Joint Meeting, Arlington, Virginia*, 2011, pp. JANNAF–672.

[9]Norris, A. T., "A-Priory Tuning of Modified Magnussen Combustion Model," *JANNAF 46th Combustion, 34th Airbreathing Joint Meeting, Newport News, Virginia*, 2016, pp. JANNAF–672.

[10]Pellett, G. L., Vaden, S. N., and Wilson, L. G., "Gaseous Surrogate Hydrocarbons for a HiFire Scramjet that Mimic Opposed Jet Extinction Limits for Cracked JP Fuels," *JANNAF 55th Propulsion Meeting, 42nd Combustion Meeting, 30th Air-Breathing Propulsion, 30th Exhaust Plume Technology, 24th Propulsion Systems Hazards and 12th Spirits Users Group Joint Subcommittee Meeting, Newton, MA*, 2008, p. JANNAF.

[11]Luo, Z., Yoo, C. S., Richardson, E. S., Chen, J. H., Law, C. K., and Lu, T. F., "Chemical Explosive Mode Analysis for a Turbulent Lifted Ethylene Jet Flame in Highly-Heated Coflow," *Combustion and Flame*, Vol. 159 (1), 2012, pp. 265–274.

[12]Hass, N., Cabell, K. F., and Storch, A. M., "HIFiRE Direct-Connect Rig (HDCR) Phase I Ground Test Results from the NASA Langley Arc-Heated Scramjet Test Facility," *JANNAF 43rd Combustion, 31st Airbreathing Joint Meeting, La Jolla, California*, 2009, pp. JANNAF–672.

[13]Cabel, K. F., Hass, N. E., Storch, A. M., and Gruber, M., "HIFiRE Direct-Connect Rig (HDCR) Phase I Scramjet Test Results from the NASA Langley Arc-Heated Scramjet Test Facility," *17th AIAA International Space Planes and Hypersonic Systems and Technologies Conference*, 2011, pp. AIAA–2011–2248.

[14]McBride, B. J., Gordon, S., and Reno, M. A., "Coefficients for Calculating Thermodynamic and Transport Properties of Individual Species," Tech. Rep. NASA Technical Memorandum 4513, NASA: Office of Management. Scientific and Technical Information Program, 1993.